

Dislocation Emission at the Silicon/Silicon Nitride Interface: A Million Atom Molecular Dynamics Simulation on Parallel Computers

Martina E. Bachlechner, Andrey Omeltchenko, Aiichiro Nakano, Rajiv K. Kalia, and Priya Vashishta

*Concurrent Computing Laboratory for Materials Simulations, Department of Physics & Astronomy
and Department of Computer Science, Louisiana State University, Baton Rouge, Louisiana 70803-4001*

Ingvar Ebbsjö

Studsvik Neutron Research Laboratory, University of Uppsala, S-611 82 Nyköping, Sweden

Anupam Madhukar

Department of Materials Science and Engineering, University of Southern California, Los Angeles, California 90089-0241

(Received 19 July 1999)

Mechanical behavior of the Si(111)/Si₃N₄(0001) interface is studied using million atom molecular dynamics simulations. At a critical value of applied strain parallel to the interface, a crack forms on the silicon nitride surface and moves toward the interface. The crack does not propagate into the silicon substrate; instead, dislocations are emitted when the crack reaches the interface. The dislocation loop propagates in the ($\bar{1}\bar{1}$) plane of the silicon substrate with a speed of 500 (\pm 100) m/s. Time evolution of the dislocation emission and nature of defects is studied.

PACS numbers: 61.72.Bb, 68.35.Gy

In silicon device technology, multilayered structures are common which involve interfaces with other materials. During the production and operation cycles, high stresses may develop at the interfaces, because of the differences in thermal and mechanical properties [1]. In multilayered materials and at interfaces this can result in crack initiation and propagation. Fracture at interfaces has been a subject of numerous experimental and theoretical studies [2–5]. Cracking patterns range from surface cracks and channeling in the film to substrate damage, spalling, and debonding of the interface. For silicon nitride, as a dielectric material and passivation layer in silicon and gallium arsenide devices it is therefore important to understand crack initiation, propagation, dislocation emission, and fracture on an atomistic level [6–8]. Molecular dynamics (MD) is a powerful method to investigate mechanical behavior of these interface systems [9–15]. A way to simulate crack initiation and its propagation is to apply uniaxial strain parallel to the interface and study time evolution of the system to analyze its failure resistance.

Our motivation is to investigate the nature of interfacial fracture at a ceramic/semiconductor interface such as silicon nitride (bulk modulus $B = 285$ GPa) or silicon ($B = 99$ GPa) using large scale MD simulations on parallel computers. The mechanical behavior of crystalline, amorphous, and nanophase silicon nitride as ceramic materials has already been studied by molecular dynamics [16]. We present here the first MD simulation of Si/Si₃N₄ interfacial fracture. Our simulations shed light on the recent experiments of Ohta *et al.* [17]. They report dislocation generation in silicon substrates at the silicon nitride/silicon edge during high-temperature fabri-

cating processes. This situation is similar to our simulation, where fractured silicon nitride generates dislocations in silicon below the crack. However, to the best of our knowledge, no direct mechanical tests of interfacial fracture on this particular system have been published.

Silicon nitride has a hexagonal structure. It occurs in two forms, alpha and beta, which are very closely related. There are four Si₃N₄ molecules per unit cell in alpha Si₃N₄. Silicon, on the other hand, has a diamond structure. Structurally, the (0001) plane of the silicon nitride is similar to the (111) plane of silicon. The 2×2 unit cell of silicon containing four atoms on the (111) plane is close to the rectangular unit cell of the (0001) plane of silicon nitride containing four nitrogen atoms—the lattice mismatch is only 1.1%, with silicon nitride being larger than silicon. Bonds are formed from each of the four nitrogen atoms at the interfacial plane of silicon nitride to the four Si atoms of the interfacial plane in silicon. Silicon atoms in the Si₃N₄ interfacial plane are threefold coordinated to the nitrogens instead of the usual fourfold in bulk Si₃N₄. This defect is experimentally well characterized in the Si/Si₃N₄ interface [8]. In the bulk silicon nitride the Si-N bond length is 1.73 Å and the Si-Si nearest-neighbor distance in silicon is 2.35 Å.

In our simulations, silicon nitride is represented by an interatomic potential involving two- and three-body interactions. The two-body terms include steric repulsion, the effect of charge transfer via Coulomb interaction, and the large electronic polarizability of anions through the charge-dipole interaction [18]. Three-body terms account for bond-bending and bond-stretching effects. Bulk and Young moduli, along with the phonon density of states of α crystal [19,20] and structural correlations in the

amorphous state [21], are well described by the interaction potential. It has been used successfully to study fracture in crystalline, amorphous, and nanophase Si_3N_4 (see Ref. [16]). The silicon system is described by the Stillinger-Weber potential [22]. To account for all of the structural correlations for silicon, silicon nitride, and the $\text{Si}(111)/\text{Si}_3\text{N}_4(0001)$ interface, the system is modeled using eight components [15]. These consist of Si^{4+} and N^{3-} in the bulk Si_3N_4 ; Si^{3+} , N^{2-} , and N^{3-} at the Si_3N_4 side of the interface; threefold coordinated Si at the $\text{Si}(111)$ interface, its fourfold coordinated neighboring silicon in the plane; and bulk Si. The million atom simulations were performed on 46 processors of the DEC alpha cluster with two gigaswitches at the Concurrent Computing Laboratory for Materials Simulations at Louisiana State University using highly efficient space-time multiresolution MD algorithms. Molecular dynamics, Langevin dynamics, and steepest descent quench methods were used. Time step in MD simulations was 3 fs.

To separate the effect of lattice mismatch between $\text{Si}(111)$ and $\text{Si}_3\text{N}_4(0001)$, a Stillinger-Weber potential of a model of silicon with a 1.1% larger lattice constant was constructed. Si-Si bonds in silicon at the interface experience different environments from silicon nitride across the interface. Si-N bond lengths in bulk silicon nitride and across the interface, along with the nearest-neighbor Si-Si distances in bulk silicon and its variation at the interface due to the presence of silicon nitride, are given in Table I. The Si-N bond lengths for threefold coordinated silicons in silicon nitride are 1.6 to 1.65 Å compared to 1.73 Å for fourfold silicons in the bulk. This is consistent with the bond-order arguments. Twofold coordinated nitrogen at the interface feels the attraction of the silicon system—its distance to bulk Si atoms in silicon nitride increases to 1.88 Å. The Si-N bond lengths across the interface, 1.68, and 1.70 Å, are close to the bulk value of 1.73 Å. From the crystal structure of silicon and from the geometry of the interface, we

TABLE I. Si-N and Si-Si bond lengths at and near the interface in silicon nitride and silicon.

	Bond lengths (Å)
Si-N bonds in Si_3N_4	1.73 (bulk) 1.60, 1.65, 1.88 (within interface layer)
Si-N interface bonds between silicon and N in Si_3N_4	1.68, 1.70
Si-Si bonds in silicon	2.35 (bulk) 2.31, 2.34, 2.36 (within interface layer) 2.35, 2.36 (between interface layer and bulk)

can clearly distinguish between three different Si-Si bond lengths in the interfacial region of silicon (2.31, 2.34, and 2.36 Å). Bonds from Si in the interface layer to Si in the bulk of silicon (these bonds are perpendicular to the interface) have two major peaks at 2.35 and 2.36 Å, because of two different environments. These interfacial bond lengths are consistent with chemical arguments and self-consistent LCAO calculations [23] and give a satisfactory description of the structure of silicon nitride/silicon interface.

Two sets of MD simulations with 210 240 atoms and with 1 121 904 atoms were carried out. In our first simulation, the dimensions of the silicon part are $162 \text{ Å} \times 233 \text{ Å} \times 38 \text{ Å}$, and the matching silicon nitride part has a height of 39 Å. A schematic of the geometry of the interface system is shown in Fig. 1. After thermalizing the system at 300 K, the system was stretched parallel to the interface, i.e., in the $[2100]$ direction for silicon nitride and in the $[\bar{2}11]$ direction for silicon, until it failed. For each percent of strain the system has been subjected to a 2 ps stretching phase and a 2 ps relaxation phase as seen in the time evolution of σ_{xx} , the stress tensor component in the stretching direction (see Fig. 2). The system did not show any failure up to 8% strain. At 9% strain, within the first 2 ps, σ_{xx} decreased dramatically. This is due to the fact that a crack started to form at the top surface of the silicon nitride layer and it propagated through the whole silicon nitride layer within 17 ps. The system was monitored for an additional 80 ps. It was found that the crack does not propagate into Si, but instead emits dislocations, which correlates well with an additional drop in σ_{xx} after 48 ps. We have examined the structure of silicon at the interface to determine the nature of defects created by the crack arriving from silicon nitride. In Fig. 3 the extra line of atoms (in yellow) in a $\text{Si}(111)$ plane parallel to the interface—an edge dislocation—can be clearly seen. The dislocation core lies within the white dashed circle. The projection of the displacement vector onto the (111) plane is in the $[1\bar{1}0]$ direction as indicated by the arrow from a red to a yellow Si atom.

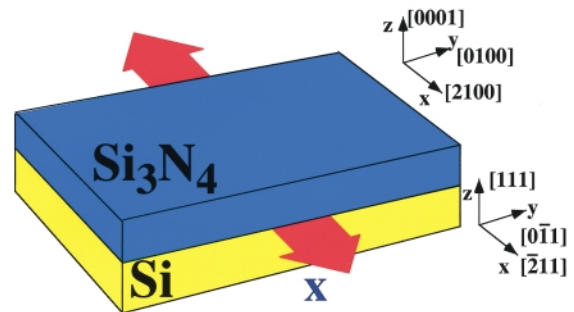


FIG. 1 (color). Schematic of fracture geometry for the $\text{Si}/\text{Si}_3\text{N}_4$ interface.

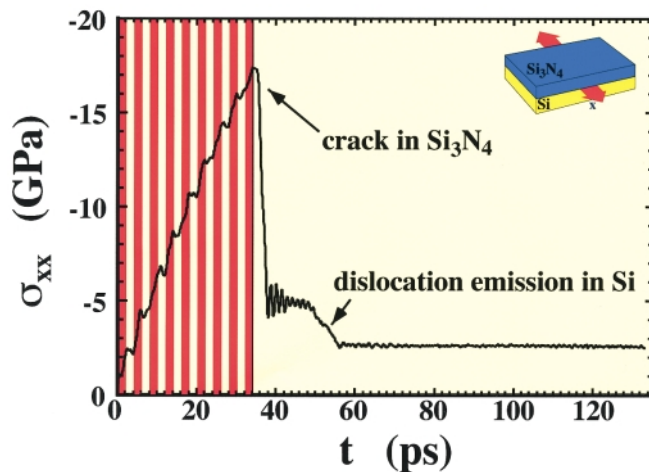


FIG. 2 (color). Time evolution of stress, σ_{xx} . The system is stretched (red) and relaxes (yellow) until 34 ps when there is a catastrophic drop in σ_{xx} , indicating crack propagation from the top surface of silicon nitride toward the interface. The second drop after 40 ps is due to dislocation emission in silicon.

To study size effects, a larger system was used in the second simulation. The system consists of 1.12 million atoms; the silicon part is now $283 \text{ \AA} \times 412 \text{ \AA} \times 67 \text{ \AA}$, and the silicon nitride film has exactly the same dimensions as the silicon part. This system failed at 8% instead of 9% for the smaller system, and the effect in the stress release was not as pronounced. This can be attributed to the creation of two cracks in the top surface of silicon nitride (see Fig. 4) for the larger system versus a single crack for the smaller system, which agrees well with the micromechanic theories of Hutchinson and Suo predicting increasing crack probabilities with increasing thickness [2]. The geometry of two cracks separated by 90 \AA

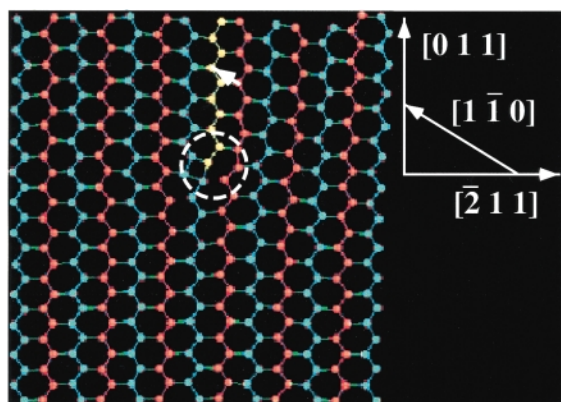


FIG. 3. (color) Atomic positions in a slice of Si(111) parallel to the interface showing the dislocation. Alternating double layers are colored red and turquoise to visualize the extra double layer shown in yellow. The core of the edge dislocation lies within the white dashed circle. The projection of the displacement vector onto the (111) plane is in the $[1\bar{1}0]$ direction as indicated by the white arrow going from a red Si atom to a yellow Si atom.

provides considerable stress relaxation in the x direction as manifested in σ_{xx} . However, both cracks propagate from the top surface of silicon nitride toward the interface and emit dislocations in silicon. The structure of this interface was also examined to determine the nature of defects by the two cracks. The highest energy is stored in the dislocation core at the end of an extra line of atoms, as indicated by the dashed circle in Fig. 3. Its time evolution is given in Figs. 5(a)–5(c). Only those Si atoms whose energies are higher than the average silicon energy by $+0.35 \text{ eV}$ are shown. Interfacial (blue) and surface atoms (red) also satisfy this criterion, i.e., their energy is 0.35 eV larger than the average energy, and can be seen at the top [interface (blue atoms)] and bottom [silicon surface (red atoms)]. In Fig. 5(a), we see the formation of a dislocation loop at the interfacial plane (blue) and the right-hand silicon surface (surface atoms belonging to the vertical planes have been removed from the plot to make the dislocation loop visible). The dislocation loop lies on a $(\bar{1}\bar{1}1)$ plane, denoted with dashed lines in Fig. 5(a). This loop has five segments; the line in the interfacial plane (blue atoms at the top) is in direction $[1\bar{1}0]$, the first segment. Moving clockwise, the second segment (vertical) is in direction $[011]$, the third in direction $[01\bar{1}]$, the fourth in direction $[110]$, and the last segment is in direction $[011]$. As time proceeds the dislocation loop grows [see Figs. 5(b) and 5(c)] until it reaches the silicon surface (red) at the bottom after 13 ps. From our simulation data we estimate the speed of the dislocation motion to be $500 (\pm 100) \text{ m/s}$.

In summary, parallel MD simulations have been performed to analyze the mechanical stability of the Si(111)/Si₃N₄(0001) system by applying uniaxial strain parallel to the interface. It is found that the system fails, starting from the top surface of silicon nitride where a

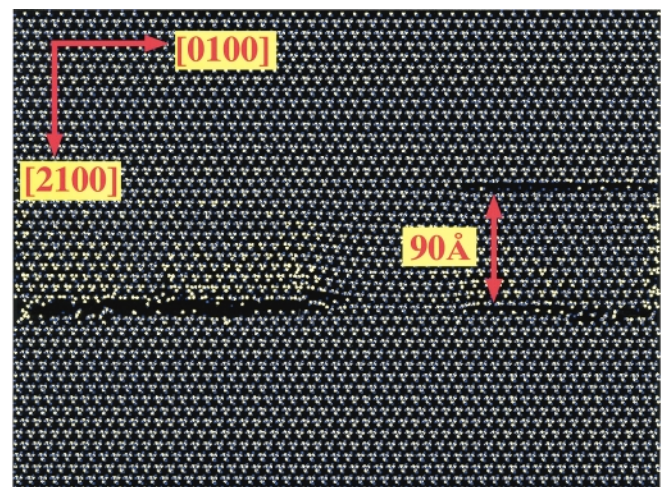


FIG. 4 (color). Atomic positions in a slice of silicon nitride parallel to the interface showing two cracks. The direction of cracks is $[0100]$.

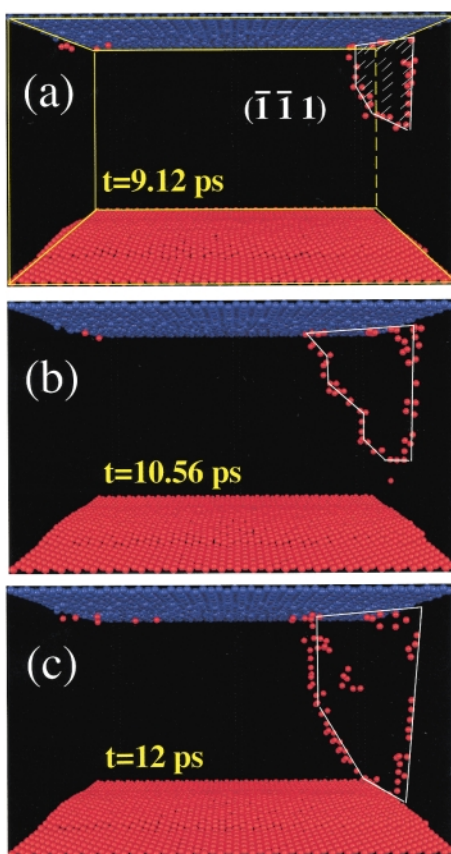


FIG. 5 (color). Time evolution of dislocation motion. Atoms with energies larger than the average silicon energy by $+0.35$ eV are plotted, i.e., interfacial atoms (blue), surface atoms (red), and atoms in the dislocation core (red). (a) Formation of a dislocation loop at the interfacial plane (blue) and the right-hand silicon surface (surface atoms belonging to the vertical planes have been removed from the plot to make the dislocation loop visible). The dislocation loop lies on a $(\bar{1}\bar{1}1)$ plane denoted with dashed lines. Five loop segments: in the interfacial plane (blue atoms at the top) in direction $[1\bar{1}0]$; moving clockwise, the second segment (vertical) in direction $[011]$, the third in direction $[01\bar{1}]$, the fourth in direction $[110]$, and the last segment is in direction $[011]$. (b),(c) Dislocation loop after 10.56 and 12 ps, respectively.

crack is created, which propagates through the whole of silicon nitride but does not propagate through silicon. Silicon does not fracture, instead dislocations are emitted which form a loop and travel to the bottom side of silicon film with a speed of about 500 m/s. The size effect of the system is also investigated. Whereas the basic mechanisms are the same as for the smaller system, more cracks originating from the larger thickness of the larger system lead to more complex defect geometries.

This work was supported by the Austrian FWF (J01146-PHY and J01444-PHY), DOE (Grant No. DE-FG02-96ER45570), NSF (Grants No. DMR-9711903

and No. ASC-9701504), AFOSR (Grants No. F 49620-99-1-0250 and No. F 49620-98-1-0086), USC-LSU MURI (Grant No. F 49620-95-1-0452), ARO (Grant No. DAAH04-96-1-0393), and PRF (Grant No. 31659-AC9). Simulations were performed on the parallel machines in the Concurrent Computing Laboratory for Materials Simulations at LSU.

-
- [1] D. K. Ferry and S. M. Goodnick, *Transport in Nanostructures* (Cambridge University Press, Cambridge, England, 1997).
 - [2] J. W. Hutchinson and Z. Suo, *Adv. Appl. Mech.* **29**, 63 (1992); A. G. Evans and J. W. Hutchinson, *Acta Metall. Mater.* **43**, 2507 (1995).
 - [3] M. D. Thouless, *IBM J. Res. Dev.* **38**, 367 (1994).
 - [4] P. Daguier *et al.*, *Phys. Rev. Lett.* **78**, 1062 (1997).
 - [5] K. Ravi-Chandar and B. Yang, *J. Mech. Phys. Solids* **45**, 535 (1997); C. M. Nygards, K. W. White, and K. Ravi-Chandar, *Thin Solid Films* **332**, 185 (1998).
 - [6] W. C. Tang *et al.*, *Appl. Phys. Lett.* **58**, 1644 (1991).
 - [7] C. Meyer *et al.*, *Phys. Rev. Lett.* **74**, 3001 (1995).
 - [8] A. Stesmans and G. V. Gorp, *Phys. Rev. B* **52**, 8904 (1995).
 - [9] C. Donati, S. C. Glotzer, and P. H. Poole, *Phys. Rev. Lett.* **82**, 5064 (1999).
 - [10] F. F. Abraham *et al.*, *Comput. Phys.* **12**, 538 (1998).
 - [11] V. Bulatov *et al.*, *Nature (London)* **391**, 669 (1998).
 - [12] Y.-M. Juan, Y. Sun, and E. Kaxiras, *Philos. Mag. Lett.* **73**, 233 (1996).
 - [13] K. T. Thomson, R. M. Wentzcovitch, and M. S. T. Bukowinski, *Science* **274**, 1880 (1996).
 - [14] S. J. Cook and P. Clancy, *Phys. Rev. B* **47**, 7686 (1993).
 - [15] M. E. Bachlechner *et al.*, *Appl. Phys. Lett.* **72**, 1969 (1998).
 - [16] A. Nakano, R. K. Kalia, and P. Vashishta, *Phys. Rev. Lett.* **75**, 3138 (1995); P. Vashishta *et al.*, *Mater. Sci. Eng. B* **37**, 56 (1996); R. K. Kalia *et al.*, *Phys. Rev. Lett.* **78**, 2144 (1997); K. Tsuruta *et al.*, *J. Am. Ceram. Soc.* **81**, 433 (1998).
 - [17] H. Ohta, H. Miura, and M. Kitano, *Mater. Sci. Res. Int.* **4**, 261 (1998).
 - [18] P. Vashishta, *et al.*, in *Amorphous Insulators and Semiconductors*, edited by M. F. Thorpe and M. I. Mitkova NATO ASI Ser., Vol. 23 (Kluwer, Dordrecht, 1996), p. 151.
 - [19] C.-K. Loong *et al.*, *Europhys. Lett.* **31**, 201 (1995).
 - [20] P. Vashishta, R. K. Kalia, and I. Ebbsjö, *Phys. Rev. Lett.* **75**, 858 (1995).
 - [21] M. Misawa *et al.*, *J. Non-Cryst. Solids* **34**, 314 (1979).
 - [22] F. H. Stillinger and T. A. Weber, *Phys. Rev. B* **31**, 5262 (1985).
 - [23] G. L. Zhao and M. E. Bachlechner, *Phys. Rev. B* **58**, 1887 (1998).